Active control of the axisymmetric vibration modes of a tom-tom drum using a modal-based observer-regulator

Marc Wijnand, Brigitte d'Andréa-Novel, Thomas Hélie, David Roze

ACTIVE CONTROL OF THE AXISYMMETRIC VIBRATION MODES OF A TOM-TOM DRUM USING A MODAL-BASED OBSERVER-REGULATOR

Marc Wijnand[1] **Brigitte d'Andréa-Novel**[1] **Thomas Hélie**[2] **David Roze**[2]
STMS (Ircam – [2]CNRS – [1]Sorbonne Université), 1 place Igor Stravinsky, 75004 Paris, France
marc.wijnand@ircam.fr

ABSTRACT

This paper deals with an application of active control of percussion instruments. Our setup consists of a tom-tom drum with a circular membrane, a cylindrical cavity and a circular rigid wall on which a loudspeaker is mounted. The current applied to the loudspeaker is controlled in order to modify the frequencies of the axisymmetric drum membrane modes.

A hybrid PDE-ODE model of the axisymmetric transverse vibration of the tom-tom membrane coupled to a cavity and a loudspeaker, and its recast version as an infinite-dimensional port-Hamiltonian system, are recalled. Furthermore, a truncated modal projection of the model is provided.

In a previous work, a control law for the loudspeaker current was designed that modifies the frequency of the first axisymmetric vibration mode of the drum membrane, using finite-time and passivity-based methods. In addition to a pressure sensor, a sensor for the transverse displacement of the drum membrane is needed to implement the control law.

In this contribution, a finite-time observer is first designed to estimate the modal transverse displacements, removing the need for a displacement sensor. A control law for the loudspeaker current is then proposed that modifies the frequencies of multiple drum membrane modes. Finally, the control law is tested numerically on a model containing a finite number of modes. Stability and robustness of the observer-regulator controller are discussed as well as spillover effects on observation and control.

1. INTRODUCTION

1.1 Active control of musical instruments

Active control of musical instruments consists in adding a control loop to an existing acoustic musical instrument that is being played by a musician. It is an example of active vibration control [1, 2] that enables the musician to enlarge his sound palette while keeping the ergonomics of the original instrument.

One can distinguish two classes of active control of musical instruments [3–7]. In *acoustical active control*, the control acts on a fluid medium. An example is the use of a loudspeaker to create destructive interference in order to cancel sound. In *structural acoustical control*, the control acts on a solid. Examples include the use of piezoelectric actuators placed on the structure of a violin, guitar or percussion instrument.

1.2 The tom-tom drum

The tom-tom drum is a directly struck membranophone. It consists of a cylindrical body with a top (*batter head*) and bottom (*resonant head*) membrane and is a standard part of a drum kit. The sound of the tom-tom drum is referred to as "indeterminately pitched" or "having a less clear pitch" [8]. The coupling between the air in the cavity and the (top) membrane improves the harmonicity of the axisymmetric vibration modes of the membrane [9], and increases the acoustical efficiency of the instrument [10].

1.3 Active control of membranophones

Active control has been applied to following percussion instruments with a membrane-cavity coupling. In [11], control of four modes of a *drumhead* was obtained. A PID controller with stabilizing feedforward part was implemented, using four accelerometers on the drumhead as sensors and four loudspeakers acting on the cavity as actuators. A *bass drum* [12] was controlled by a negative feedback, using a piezoceramic sensor attached to the rim to measure the membrane deflection and a single loudspeaker as actuator. A *conga* [13] was endowed with a contact microphone attached to the membrane as sensor and a single loudspeaker used as actuator enables to modify the instrument's frequency response. Feedback of a piezoelectric sensor placed on the batter head of a *tom-tom drum* [14] was applied on the resonant head by an electromagnetic actuator. A pickup dynamic microphone was placed inside an electromagnetic actuator placed on the batter head of a *bass drum* in [15]. Recently, a *snare drum* [16] was controlled using an optical sensor on the batter head, and multiple actuators: two tactile transducers on the resonant head, and an additional loudspeaker on a frame mounted inside the cavity.

Our contribution focuses on the use of finite-time control methods [17], offering advantages regarding time constraints and robustness.

2. MODEL

The model as presented in [18] is recalled here: a physical model (Subsection 2.1) is recast as a Port-Hamiltonian System (Subsection 2.2). After a nondimensionalization (Subsection 2.3), the model order of the inifinite-dimensional model is reduced to N modes in Subsection 2.4. Finally, a state-space representation of the model is given in Subsection 2.5 and simulated in Subsection 2.6.

2.1 Physical model

The tom-tom drum consisting of the top membrane coupled to the cavity and loudspeaker is depicted in Figure 1. The three subsystems are modeled as explained in Subsubsections 2.1.1-2.1.3. We also comment on the spatial eigenmodes of the membrane coupled to the cavity in Subsubsection 2.1.4.

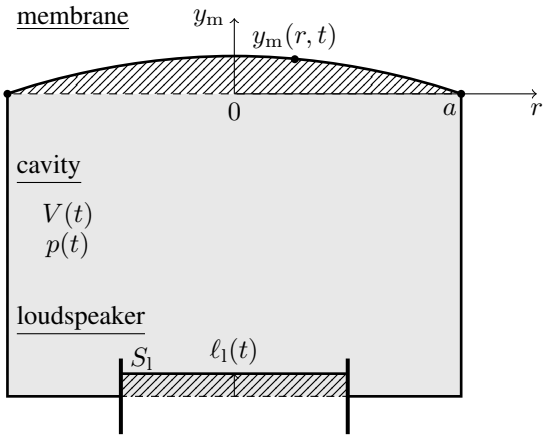

Figure 1. Geometry of the system

2.1.1 Membrane

It is supposed that the membrane executes small vertical displacements and that its tension is uniform. Furthermore, the vibration of the membrane contains only axisymmetric modes[1].

One can then state the wave equation with a pressure source as [19]

$$T\boldsymbol{\Delta} y_\mathrm{m}(r,t) + p_\mathrm{c}(t) = \sigma_\mathrm{m}\frac{\partial^2}{\partial t^2}y_\mathrm{m}(r,t) + \mu\frac{\partial}{\partial t}y_\mathrm{m}(r,t), \quad (1)$$

where $\boldsymbol{\Delta} = \frac{\partial^2}{\partial r^2} + \frac{1}{r}\frac{\partial}{\partial r}$ in polar coordinates, $y_\mathrm{m}(r,t)$ is the transverse displacement of the membrane, T is the tension $[\mathrm{N/m}]$, $\sigma_\mathrm{m} = \sigma + 0.85a\rho_\mathrm{air}$ is the equivalent areal density $[\mathrm{kg/m^2}]$ representing the sound radiation in air by the membrane [20] (σ being the membrane's areal density, a the membrane's radius and ρ_air the volumetric density of air), μ is a friction coefficient $\left[\mathrm{kg/m^2 s}\right]$ and p_c is the net pressure [Pa] applied to the membrane. The wave velocity in the membrane is $c = \sqrt{T/\sigma_\mathrm{m}}$.

The boundary condition is $y_\mathrm{m}(a,t) = 0$ (membrane clamped at rim). The initial condition representing a stroke with a mallet is $\frac{\partial y}{\partial t}(r,0) = -V_0\mathbb{I}_\varepsilon(r)\delta(0)$, with amplitude V_0 $\left[\frac{\mathrm{m}}{\mathrm{s}}\right]$, $\mathbb{I}_\varepsilon(r)$ a smooth function that varies between a value 1 for $r = 0$ and 0 for $r \geq \varepsilon$, and $\delta(0)$ the Dirac delta function at $t = 0$.

2.1.2 Cavity

Under the hypothesis of a lumped parameter acoustic model without propagation, and thus uniform pressure inside the cavity, with the air inside the cavity behaving as an ideal gas that is compressed adiabatically, one can use the approximate first order relation

$$\frac{p_\mathrm{c}}{p_0} = -\gamma\frac{V_\mathrm{c}}{V_0}, \quad (2)$$

where γ is the heat capacity ratio and the acoustical quantities p_c and V_c are the deviation values of the instantaneous pressure p and volume V with respect to the values p_0 and V_0 at rest:

$$\begin{cases} p_\mathrm{c} = p - p_0 \\ V_\mathrm{c} = V - V_0. \end{cases}$$

The two contributions to the volume change V_c are hatched in Figure 1. There is a volume change due to the transverse movement of the upper membrane and a volume change due to the position of the loudspeaker membrane, which is modeled by a plane piston of vertical position ℓ_l and effective surface S_l. Therefore,

$$V_\mathrm{c}(t) = \int_\mathcal{S} y_\mathrm{m}(r,t)\,\mathrm{d}\mathcal{S}(r) - S_\mathrm{l}\ell_\mathrm{l}(t), \quad (3)$$

with $\mathrm{d}\mathcal{S}(r) = 2\pi r\,\mathrm{d}r$, $r \in [0,a]$. Substituting (3) in (2) yields

$$p_c(t) = -\gamma\frac{p_0}{V_0}\left[\int_\mathcal{S} y_\mathrm{m}(r,t)\,\mathrm{d}\mathcal{S}(r) - S_\mathrm{l}\ell_\mathrm{l}(t)\right]. \quad (4)$$

2.1.3 Loudspeaker

The loudspeaker is modeled as a rigid disc of area S_l (plane piston, operating above its resonance frequency). The force balance on this disc yields

$$m_\mathrm{l}\ddot{\ell}_\mathrm{l}(t) + c_\mathrm{l}\dot{\ell}_\mathrm{l}(t) + k_\mathrm{l}\ell_\mathrm{l}(t) = S_\mathrm{l}p_c(t) + Bli_\mathrm{l}(t). \quad (5)$$

The left-hand side represents the forces of a standard mass-spring-damper system. The pressure in the cavity exerts a force $S_\mathrm{l}p_\mathrm{c}(t)$ on the loudspeaker membrane. The controlled current $i_\mathrm{l}(t)$ induces a Laplace force $Bli_\mathrm{l}(t)$, with B the magnetic field [T] and l [m] the length of the loudspeaker coil inside the magnetic field.

2.1.4 Spatial eigenmodes

Substituting (4) in (1) and setting $\mu = 0$ and $\ell_\mathrm{l}(t) = 0$ yields a PDE for the movement of an undamped membrane coupled to the cavity without the controlled loudspeaker:

$$c^2\boldsymbol{\Delta} y_\mathrm{m}(r,t) - \frac{\partial^2}{\partial t^2}y_\mathrm{m}(r,t) = \frac{\gamma p_0}{\sigma_\mathrm{m}V_0}\int_\mathcal{S} y_\mathrm{m}(r,t)\,\mathrm{d}\mathcal{S}(r). \quad (6)$$

In [21], it is shown that for (6), the displacement $y_\mathrm{m}(r,t)$ can be written as $y_\mathrm{m}(r,t) = \sum_{n=1}^{+\infty}\varphi_n(r)z_n(t)$ with axisymmetric eigenfunctions

$$\varphi_n(r) = w_n\left[J_0(\lambda_n r) - J_0(\lambda_n a)\right], \quad (7)$$

where $J_i(\cdot)$ is the Bessel function of the first kind of order i and w_n an arbitrary weight coefficient. It can be shown (see [21]) that the wave number λ_n satisfies the implicit condition

$$\lambda_n^2 a^2 J_0(\lambda_n a) = -\tfrac{\pi a^4\gamma p_0}{TV_0}J_2(\lambda_n a) \triangleq -BJ_2(\lambda_n a), \quad (8)$$

where the dimensionless quantity B can be interpreted as the ratio of the restoring force applied by the air in the cavity to the membrane tension [20].

[1] We suppose that the musician excites the membrane at its center. We do not consider modes with nodal lines here, for which there is no influence of the cavity.

$$\frac{\partial}{\partial t}\begin{bmatrix}\pi_{\mathrm{m}}\\ \varepsilon_{\mathrm{m}}\\ \hline V_{\mathrm{c}}\\ \hline \pi_{\mathrm{l}}\\ \ell_{\mathrm{l}}\end{bmatrix} = \left(\left[\begin{array}{ccc|c|cc} 0 & \mathrm{div} & -\mathbb{1} & 0 & 0\\ \mathrm{grad} & 0 & 0 & 0 & 0\\ \hline \int_{\mathcal{S}}\cdot\,\mathrm{d}\mathcal{S} & 0 & 0 & -S_{\mathrm{l}} & 0\\ \hline 0 & 0 & S_{\mathrm{l}} & 0 & -1\\ 0 & 0 & 0 & 1 & 0\end{array}\right] - \left[\begin{array}{cc|c|cc} \mu & 0 & 0 & 0 & 0\\ 0 & 0 & 0 & 0 & 0\\ \hline 0 & 0 & 0 & 0 & 0\\ \hline 0 & 0 & 0 & c_{\mathrm{l}} & 0\\ 0 & 0 & 0 & 0 & 0\end{array}\right]\right)\begin{bmatrix}\frac{\pi_{\mathrm{m}}}{\sigma_{\mathrm{m}}}\\ T\varepsilon_{\mathrm{m}}\\ \hline \frac{E_0}{V_{\mathrm{c}}^2}V_{\mathrm{c}}\\ \hline \frac{\pi_{\mathrm{l}}}{m_{\mathrm{l}}}\\ k_{\mathrm{l}}\ell_{\mathrm{l}}\end{bmatrix} + \begin{bmatrix}0\\ 0\\ \hline 0\\ \hline Bl\\ 0\end{bmatrix} i_{\mathrm{l}} \tag{9}$$

$$\frac{\partial}{\partial \tilde{t}}\begin{bmatrix}\tilde{\pi}_{\mathrm{m}}\\ \tilde{\varepsilon}_{\mathrm{m}}\\ \hline \tilde{V}_{\mathrm{c}}\\ \hline \tilde{\pi}_{\mathrm{l}}\\ \tilde{\ell}_{\mathrm{l}}\end{bmatrix} = \left(\left[\begin{array}{ccc|c|cc} 0 & \left(\frac{\partial}{\partial \tilde{r}}+\frac{1}{\tilde{r}}\right) & -\alpha\mathbb{1} & 0 & 0\\ \frac{\partial}{\partial \tilde{r}} & 0 & 0 & 0 & 0\\ \hline \alpha\int_{\tilde{\mathcal{S}}}\cdot\,\mathrm{d}\tilde{\mathcal{S}} & 0 & 0 & -\beta_1 & 0\\ \hline 0 & 0 & \beta_1 & 0 & -\beta_2\\ 0 & 0 & 0 & \beta_2 & 0\end{array}\right] - \left[\begin{array}{cc|c|cc} \xi & 0 & 0 & 0 & 0\\ 0 & 0 & 0 & 0 & 0\\ \hline 0 & 0 & 0 & 0 & 0\\ \hline 0 & 0 & 0 & \zeta & 0\\ 0 & 0 & 0 & 0 & 0\end{array}\right]\right)\begin{bmatrix}\tilde{\pi}_{\mathrm{m}}\\ \tilde{\varepsilon}_{\mathrm{m}}\\ \hline \tilde{V}_{\mathrm{c}}\\ \hline \tilde{\pi}_{\mathrm{l}}\\ \tilde{\ell}_{\mathrm{l}}\end{bmatrix} + \begin{bmatrix}0\\ 0\\ \hline 0\\ \hline 1\\ 0\end{bmatrix}\tilde{i}_{\mathrm{l}} \tag{10}$$

$$\frac{\mathrm{d}}{\mathrm{d}\tilde{t}}\begin{bmatrix}\tilde{z}_1\\ \tilde{z}_2\\ \partial_{\tilde{t}}\tilde{z}_1\\ \partial_{\tilde{t}}\tilde{z}_2\\ \hline \tilde{V}_{\mathrm{c}}\\ \hline \tilde{\pi}_{\mathrm{l}}\\ \tilde{\ell}_{\mathrm{l}}\end{bmatrix} = \left(\left[\begin{array}{cccc|c|cc} 0 & 0 & \frac{1}{\kappa^2} & 0 & 0 & 0 & 0\\ 0 & 0 & 0 & \frac{1}{\kappa^2} & 0 & 0 & 0\\ -\frac{1}{\kappa^2} & 0 & 0 & 0 & \frac{\sqrt{\pi}\alpha}{\kappa B\chi_{I,1}}\tilde{\lambda}_1\mathrm{sign}\left(J_0(\tilde{\lambda}_1)\right) & 0 & 0\\ 0 & -\frac{1}{\kappa^2} & 0 & 0 & \frac{\sqrt{\pi}\alpha}{\kappa B\chi_{I,2}}\tilde{\lambda}_2\mathrm{sign}\left(J_0(\tilde{\lambda}_2)\right) & 0 & 0\\ \hline 0 & 0 & -\frac{\sqrt{\pi}\alpha}{\kappa B\chi_{I,1}}\tilde{\lambda}_1\mathrm{sign}\left(J_0(\tilde{\lambda}_1)\right) & -\frac{\sqrt{\pi}\alpha}{\kappa B\chi_{I,2}}\tilde{\lambda}_2\mathrm{sign}\left(J_0(\tilde{\lambda}_2)\right) & 0 & -\beta_1 & 0\\ \hline 0 & 0 & 0 & 0 & \beta_1 & 0 & -\beta_2\\ 0 & 0 & 0 & 0 & 0 & \beta_2 & 0\end{array}\right] - \left[\begin{array}{cccc|c|cc} 0 & 0 & 0 & 0 & 0 & 0 & 0\\ 0 & 0 & 0 & 0 & 0 & 0 & 0\\ 0 & 0 & \frac{\xi}{\kappa^2} & 0 & 0 & 0 & 0\\ 0 & 0 & 0 & \frac{\xi}{\kappa^2} & 0 & 0 & 0\\ \hline 0 & 0 & 0 & 0 & 0 & 0 & 0\\ \hline 0 & 0 & 0 & 0 & 0 & \zeta & 0\\ 0 & 0 & 0 & 0 & 0 & 0 & 0\end{array}\right]\right)\cdots$$

$$\cdots\left[\begin{array}{cccc|c|cc} \kappa^2\tilde{\lambda}_1^2\frac{\chi_{I,1}^2}{\chi_{I,1}^2} & -\frac{\kappa^2}{B}\frac{\tilde{\lambda}_1\tilde{\lambda}_2}{\chi_{I,1}\chi_{I,2}}\mathrm{sign}\left(J_0(\tilde{\lambda}_1)\right)\mathrm{sign}\left(J_0(\tilde{\lambda}_2)\right) & 0 & 0 & 0 & 0 & 0\\ -\frac{\kappa^2}{B}\frac{\tilde{\lambda}_1\tilde{\lambda}_2}{\chi_{I,1}\chi_{I,2}}\mathrm{sign}\left(J_0(\tilde{\lambda}_1)\right)\mathrm{sign}\left(J_0(\tilde{\lambda}_2)\right) & \kappa^2\tilde{\lambda}_2^2\frac{\chi_{I,2}^2}{\chi_{I,2}^2} & 0 & 0 & 0 & 0 & 0\\ 0 & 0 & \kappa^2 & 0 & 0 & 0 & 0\\ 0 & 0 & 0 & \kappa^2 & 0 & 0 & 0\\ \hline 0 & 0 & 0 & 0 & 1 & 0 & 0\\ \hline 0 & 0 & 0 & 0 & 0 & 1 & 0\\ 0 & 0 & 0 & 0 & 0 & 0 & 1\end{array}\right]\begin{bmatrix}\tilde{z}_1\\ \tilde{z}_2\\ \partial_{\tilde{t}}\tilde{z}_1\\ \partial_{\tilde{t}}\tilde{z}_2\\ \hline \tilde{V}_{\mathrm{c}}\\ \hline \tilde{\pi}_{\mathrm{l}}\\ \tilde{\ell}_{\mathrm{l}}\end{bmatrix} + \begin{bmatrix}0\\ 0\\ 0\\ 0\\ \hline 0\\ \hline 1\\ 0\end{bmatrix}\tilde{i}_{\mathrm{l}} \tag{11}$$

2.2 Port-Hamiltonian reformulation

In the Port-Hamiltonian System (PHS, [22, 23]) framework, a system is modeled as consisting of three types of elementary components: energy-storing components, energy-dissipating components and external components. A PHS model satisfies the power balance. Within this framework, stable simulation [24] and control [25] methods can be developed.

In [18], the hybrid PDE-ODE system consisting (1)-(4)-(5) was recast as a PHS. The result of this reformulation is repeated here.

Definition 1 (Infinite-dimensional PHS)**.** *An infinite-dimensional PHS is defined as [26, 27]*

$$\begin{cases}\partial_t\boldsymbol{x} = (\mathcal{J}-\mathcal{R})\delta_{\boldsymbol{x}}\mathcal{H}(\boldsymbol{x}) + \mathcal{G}\boldsymbol{u}\\ \quad\boldsymbol{y} = \mathcal{G}^*\delta_{\boldsymbol{x}}\mathcal{H}(\boldsymbol{x})\end{cases} \tag{12}$$

where

- $\mathbb{X}$ *is the energy state space,*
- $\boldsymbol{u}$ *and* $\boldsymbol{y}$ *are the input and its associated output,*
- *a scalar product* $\langle\cdot,\cdot\rangle_{\mathbb{X}}$ *and norm* $\|\cdot\|_{\mathbb{X}}$ *are defined,*
- *the Hamiltonian function is obtained as* $\mathcal{H}(\boldsymbol{x}) \triangleq \frac{1}{2}\|\boldsymbol{x}\|_{\mathbb{X}}^2$,
- *the operator* $\delta_{\boldsymbol{x}}$ *is the variational derivative [28],*
- *the operator* $\mathcal{J}$ *is formally skew-symmetric and the operator* $\mathcal{R}$ *is non-negative symmetric, w.r.t. the scalar product,*
- $\mathcal{G}$ *is an operator and* $\mathcal{G}^*$ *its adjoint operator.*

The first equation of the PHS model is shown in Eq. (9) above. The state $\boldsymbol{x}$ consists of the areal momentum of the membrane $\pi_{\mathrm{m}}(\triangleq \sigma_{\mathrm{m}}\dot{y}_{\mathrm{m}})$ and its strain $\varepsilon_{\mathrm{m}}(\triangleq \boldsymbol{\nabla}y_{\mathrm{m}})$, the incremental volume of the cavity V_{c}, the loudspeaker membrane's momentum $\pi_{\mathrm{l}}(\triangleq m_{\mathrm{l}}\dot{\ell}_{\mathrm{l}})$ and its vertical position ℓ_{l}. Furthermore, $E_0 = \gamma p_0 V_0$, $\mathbb{1}$ is the identity operator, $\mathrm{grad} = \frac{\partial}{\partial r}$ and $\mathrm{div} = \left(\frac{\partial}{\partial_r}+\frac{1}{r}\right)$.

The output equation of the PHS model corresponds to $\boldsymbol{y} = \mathcal{G}^\intercal\partial_{\boldsymbol{x}}\mathcal{H}(\boldsymbol{x}) = Bl\dot{\ell}_{\mathrm{l}} \triangleq u_{\mathrm{l}}$, the electromotive force. Note that the product between input i_{l} and output u_{l} represents the electrical power supplied to the loudspeaker of the system. This output equation of the PHS will not be considered in the remainder of the paper.

2.3 Nondimensionalization

We nondimensionalize the PHS model in order to simplify subsequent calculations, using the transformations shown in Table 1. We thus obtain the dimensionless PHS shown in Eq. (10) above with $\mathrm{d}\tilde{\mathcal{S}} = 2\pi\tilde{r}\,\mathrm{d}\tilde{r}$, $\tilde{r}\in\tilde{\Omega} = [0,1]$.

$\tilde{r}=\frac{r}{a}$	$\tilde{t}=\frac{c}{a}t$	$\tilde{\mathcal{S}}=\frac{\mathcal{S}}{a^2}$
$\tilde{\pi}_{\mathrm{m}}=\frac{\pi_{\mathrm{m}}}{a^{-1}\sqrt{\sigma_{\mathrm{m}}\gamma p_0 V_0}}$	$\tilde{\varepsilon}_{\mathrm{m}}=\frac{\varepsilon_{\mathrm{m}}}{a^{-1}\sqrt{\gamma p_0 V_0 T^{-1}}}$	$\tilde{V}_{\mathrm{c}}=\frac{V_{\mathrm{c}}}{V_0}$
$\tilde{\pi}_{\mathrm{l}}=\frac{\pi_{\mathrm{l}}}{\sqrt{m_{\mathrm{l}}\gamma p_0 V_0}}$	$\tilde{\ell}_{\mathrm{l}}=\frac{\ell_{\mathrm{l}}}{\sqrt{k_{\mathrm{l}}^{-1}\gamma p_0 V_0}}$	$\tilde{\mathcal{H}}=\frac{\mathcal{H}}{\gamma p_0 V_0}$
$\tilde{i}_{\mathrm{l}}=\frac{i_{\mathrm{l}}}{c(aBl)^{-1}\sqrt{m_{\mathrm{l}}\gamma p_0 V_0}}$	$\zeta=\frac{ac_{\mathrm{l}}}{cm_{\mathrm{l}}}$	$\xi=\frac{\mu a}{c\sigma_{\mathrm{m}}}$
$\alpha=\frac{a^2}{c}\sqrt{\frac{\gamma p_0}{\sigma_{\mathrm{m}}V_0}}$	$\beta_1=\frac{aS_{\mathrm{l}}}{c}\sqrt{\frac{\gamma p_0}{m_{\mathrm{l}}V_0}}$	$\beta_2=\frac{a}{c}\sqrt{\frac{k_{\mathrm{l}}}{m_{\mathrm{l}}}}$
$\tilde{p}_{\mathrm{c}}=\frac{p_{\mathrm{c}}}{p_0}$	$\tilde{y}_{\mathrm{m}}=\frac{y_{\mathrm{m}}}{a}$	$\tilde{\varphi}_n=\varphi_n$
$\tilde{z}_n=\frac{z_n}{a}$	$\tilde{\lambda}_n=a\lambda_n$	$\tilde{f}=\frac{a}{c}f$

Table 1. Nondimensionalization of variables and constants

2.4 Model order reduction

We now project the infinite-dimensional part of the (dimensionless) PHS (10) on the orthonormal basis formed

by the eigenfunctions $\tilde{\varphi}_n(\tilde{r})$, (7), of the membrane coupled to the cavity[2]. Truncating at the first N modes[3], the position of the membrane $\tilde{y}_{\mathrm{m}}(\tilde{r},\tilde{t})$ is approximated as the finite sum $\tilde{y}_{\mathrm{m}}\left(\tilde{r},\tilde{t}\right) \approx \sum_{n=1}^{N} \tilde{\varphi}_n\left(\tilde{r}\right)\tilde{z}_n\left(\tilde{t}\right)$, where $\tilde{z}_n(\tilde{t})$ are the temporal evolutions corresponding to the eigenfunctions.

In this manner, a finite-dimensional approximative (dimensionless) PHS is obtained, that is shown for the case $N = 2$ in Eq. (11) above[4].

2.5 State-space representation

The $(2N+1)^{\text{th}}$ line of the truncated PHS model (11) represents the projected version

$$\frac{1}{\gamma}\tilde{p}_{\mathrm{c}}(\tilde{t}) = \sum_{i=1}^{N} \frac{\sqrt{\pi}\alpha\kappa}{B\chi_{I,i}}\tilde{\lambda}_i \mathrm{sign}\left(J_0(\tilde{\lambda}_i)\right)\tilde{z}_i(\tilde{t}) + \frac{\beta_1}{\beta_2}\tilde{\ell}_{\mathrm{l}}(\tilde{t}) \quad (13)$$

of the static cavity equation (4). This algebraic relation is instanteneous and thus redundant. It can be removed from the SHP (11) that can be rewritten in the classical state-space form

$$\begin{cases} \dot{\boldsymbol{x}} = \boldsymbol{A}\boldsymbol{x} + \boldsymbol{B}u \\ y = \boldsymbol{C}\boldsymbol{x}. \end{cases} \quad (14)$$

Here, the state $\boldsymbol{x} \in \mathbb{R}^{2N+2}$ corresponds to the state used in (11) from which the variable $\tilde{V}_{\mathrm{c}}$ (related to $\tilde{p}_{\mathrm{c}}$) has been removed. The system input u is the loudspeaker current $\tilde{i}(\tilde{t})$, and the system output y is the physical measurement of the pressure $\tilde{p}_{\mathrm{c}}(\tilde{t})$.

This representation will be used for the design of the observer in Section 4.

2.6 Simulation

The tom-tom model (14) with zero initial state exept for $\partial_{\tilde{t}}\tilde{z}_i = -0.001$ and model parameters $B = 5.54$, $\kappa = 0.171$, $\gamma = 1.4$, $\alpha = 1.33$, $\beta_1 = 0.768$, $\beta_2 = 0.353$, $\zeta = 0.0923$, $\xi = 0.1$ is considered as a running example. The time evolution of its state will be simulated[5] for different control inputs.

We start by a simulation of the case of a truncation of the model at $N = 2$ modes and without control (Fig. 2). It is observed that the simulated membrane displacement in the center $\tilde{y}(\tilde{r}=0,\tilde{t})$ contains three frequencies: two frequencies corresponding to the two membrane modes, and the lower resonance frequency of the loudspeaker that is moving freely.

[2] After definition of a scalar product $\langle\tilde{\varphi}_i,\tilde{\varphi}_j\rangle_{\mathrm{P}} \triangleq \int_{\tilde{\mathcal{S}}}\tilde{\varphi}_i\tilde{\varphi}_j\,\mathrm{d}\tilde{\mathcal{S}}\left(\tilde{r}\right)$ used for the projection, one can prove orthogonality and normalization (given a suited choice of the weights w_n).

[3] Note that the lowest-order modes are most important for the produced sound [20]. Furthermore, these modes are influenced the most by the coupling with the cavity [21].

[4] Here, $\kappa \triangleq a\sqrt{T(\gamma p_0 V_0)^{-1}}$, $\chi_{I,i} \triangleq \sqrt{\frac{\tilde{\lambda}_i^4}{4B^2} - \frac{\tilde{\lambda}_i^2}{2B} + \frac{1}{4} + \frac{2}{B}}$ and $\chi_{II,i} \triangleq \sqrt{\frac{\tilde{\lambda}_i^4}{4B^2} - \frac{\tilde{\lambda}_i^2}{2B} + \frac{1}{4} + \frac{1}{B}}$.

[5] Simulations are obtained using the Adams/BDF method with automatic stiffness detection and switching [29], with a time step $\Delta\tilde{t} = 0.001$.

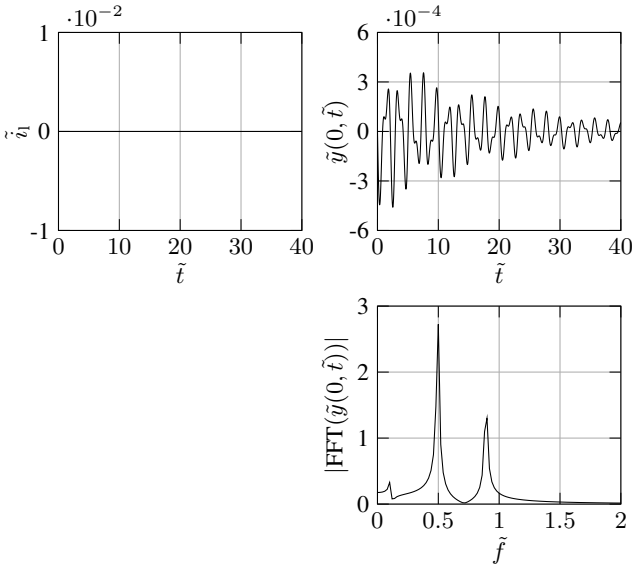

Figure 2. Simulation of the uncontrolled system with $N = 2$ modes

3. PASSIVE FINITE-TIME CONTROL OF THE N-MODAL MODEL

The control goal is to modify the frequencies of the first N axisymmetric vibration modes ($\tilde{z}_i$) of the tom-tom membrane. To this means, we first develop a control loop that controls the loudspeaker current $\tilde{i}_{\mathrm{l}}$ based on a measurement of the pressure $\tilde{p}_{\mathrm{c}}$ inside the cavity and of the temporal evolutions $\tilde{z}_i$ of the first N modes. By changing the vertical position of the loudspeaker, the volume and thus pressure inside the cavity are changed. This pressure acts on the tom-tom membrane and influences its vibrational behaviour.

The synthesis of this controller based on the projected model with N modes (14) consists of 3 steps: a pole placement on the membrane, the use of the coupling between the three subsystems, and a finite-time position control of the loudspeaker. It is a direct generalization of the control of the frequency of the first mode that was presented in [18].

3.1 Control of the membrane by pole placement

The first $2N$ equations of the model (11) represent the vibration of the first N axisymmetric modes of the circular membrane subjected to a distributed pressure $\tilde{p}_{\mathrm{c}}$ that is seen as an intermediate control input. This subsystem being controllable, if we can make the pressure satisfy

$$\tilde{p}_{\mathrm{c}}^{*}\left(\tilde{t}\right) = -\sum_{i=1}^{N}\left[k_{i,a}\tilde{z}_i\left(\tilde{t}\right) + k_{i,b}\partial_{\tilde{t}}\tilde{z}_i\left(\tilde{t}\right)\right], \quad (15)$$

where $k_{i,a}$ and $k_{i,b}$ are parameters to be determined by a pole placement, we obtain desired frequencies and damping coefficients of the first N modes. In this notation, the asterisk represents a desired trajectory.

3.2 Coupling between the three subsystems

The static relation (13) provides a link between the temporal evolutions $\tilde{z}_i$ of the first N membrane modes, the

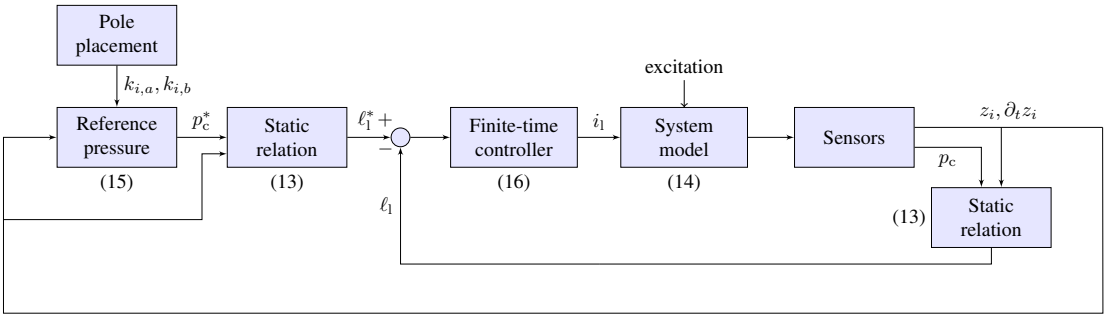

Figure 3. Control layout of the finite-time control of the N-modal model. Corresponding equations are indicated.

pressure in the cavity $\tilde{p}_c$ and the loudspeaker position $\tilde{\ell}_1$.

If we substitute $\tilde{p}_c$ with a pressure measurement $\tilde{p}_c^m$ and $\tilde{z}_i$ with amplitude measurements $\tilde{z}_i^m$ in this static relation, we can calculate an (implicit) *measurement* for the loudspeaker position: $\tilde{\ell}_1 \triangleq \tilde{\ell}_1^m$.

On the other hand, if we substitute $\tilde{p}_c$ with the pressure reference p_c^* as obtained by the pole placement in (15), while still substituting $\tilde{z}_i$ with amplitude measurements $\tilde{z}_i^m$ in this static relation, we can calculate a *reference* for the loudspeaker position: $\tilde{\ell}_1 \triangleq \tilde{\ell}_1^*$.

In this fashion, a pressure error $\tilde{p}_c^m - \tilde{p}_c^*$ is rewritten as a position error $\tilde{\ell}_1^m - \tilde{\ell}_1^*$, that will be used in the design of a finite-time position controller of the loudspeaker in the next subsection.

3.3 Finite-time position control of the loudspeaker

3.3.1 Finite-time control

A system controlled in finite time will reach an equilibrium point in a finite time. A more formal definition of finite-time stability is given in [17, Def. 2.2].

3.3.2 Finite-time control law for the loudspeaker current

In [30,31], we have shown how an existing finite-time control law of a double integrator [32] can be used to formulate a passive[6] law for the loudspeaker current in order to control its position $\tilde{\ell}_1(\tilde{t})$ to a reference trajectory $\tilde{\ell}_1^*(\tilde{t})$ in finite time.

In our case, this corresponds to the control law

$$\tilde{i}_1 = \tfrac{\beta_1}{\gamma}\tilde{p}_c^m + \beta_2\tilde{\ell}_1^m + \tfrac{\zeta}{\beta_2}\partial_{\tilde{t}}\tilde{\ell}_1^m - \bar{k}_3\left(\tilde{\ell}_1^m - \tilde{\ell}_1^*\right) - \bar{k}_4\left(\partial_{\tilde{t}}\tilde{\ell}_1^m - \partial_{\tilde{t}}\tilde{\ell}_1^*\right) - \tfrac{1}{\beta_2}\left(\bar{k}_1\left\lfloor\tilde{\ell}_1^m - \tilde{\ell}_1^*\right\rceil^{\frac{\bar{\alpha}}{2-\bar{\alpha}}} + \bar{k}_2\left\lfloor\partial_{\tilde{t}}\tilde{\ell}_1^m - \partial_{\tilde{t}}\tilde{\ell}_1^*\right\rceil^{\bar{\alpha}}\right), \quad (16)$$

with control parameters $\bar{k}_1, \bar{k}_2 > 0$, $\bar{\alpha} \in]0,1[$, $\bar{k}_3 > \beta_2$, $\bar{k}_4 > \frac{\zeta}{\beta_2}$. The expressions for the signals $\tilde{\ell}_1^m$ and $\tilde{\ell}_1^*$ (and their time derivatives) were given in Subsection 3.2.

Using this control law, we can achieve the desired pressure p_c^* ensuring the pole placement of the upper membrane. The total control structure is shown in Fig. 3 above. It consists of a fast (finite-time) control loop that tracks a slowly (asymptotically) varying reference pressure. By Tikhonov's theorem, stability of this cascade structure is ensured.

[6] A passive version of the controller was proposed, in the sense that it can be reinterpreted as a PHS and as such provides robustness against bad parameter estimation.

3.4 Simulation

The finite-time control law (16) with parameters $\bar{k}_1 = \bar{k}_2 = 10$, $\bar{k}_3 = 2\beta_2$, $\bar{k}_4 = 2\zeta/\beta_2$, $\bar{\alpha} = 0.9$ is now applied to the system, considering $N = 2$ modes. It is assumed that the entire state is known. The pole placement was calculated in order to obtain a frequency ratio of $\tilde{f}_2 : \tilde{f}_1 = 2:1$ for the two membrane modes, corresponding to parameters $k_{1a} = 0.3$, $k_{2a} = -0.7$, $k_{1b} = k_{2b} = 0$. The resulting frequency shifts are observed in Fig. 4.

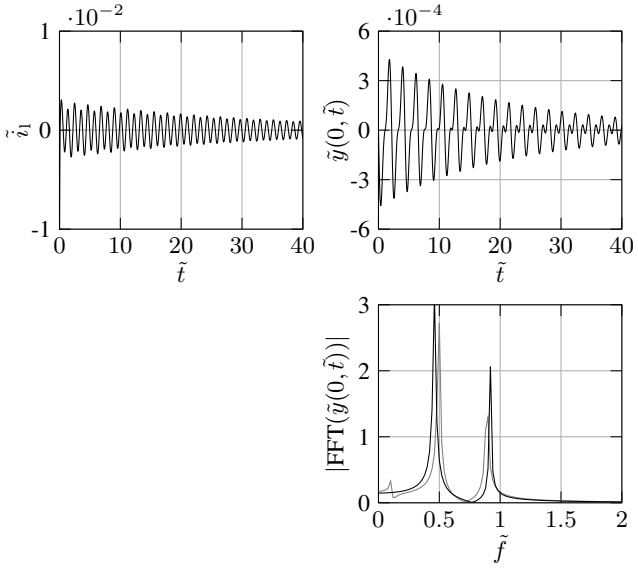

Figure 4. Simulation of the system with $N = 2$ with the finite-time controller. The spectrum for the case without control (see Fig. 2) is drawn in gray as a comparison.

4. FINITE-TIME OBSERVER

4.1 Principle

The control law (16) contains the measurement of the modal displacements $\tilde{z}_i$ of the membrane. However, this measurement is often difficult to achieve in practice. Therefore, an observer is designed, that reconstructs the entire state from the sole measurement of the pressure $\tilde{p}_c$, the system being observable. The structure of the resulting observer-regulator is shown in Fig. 5.

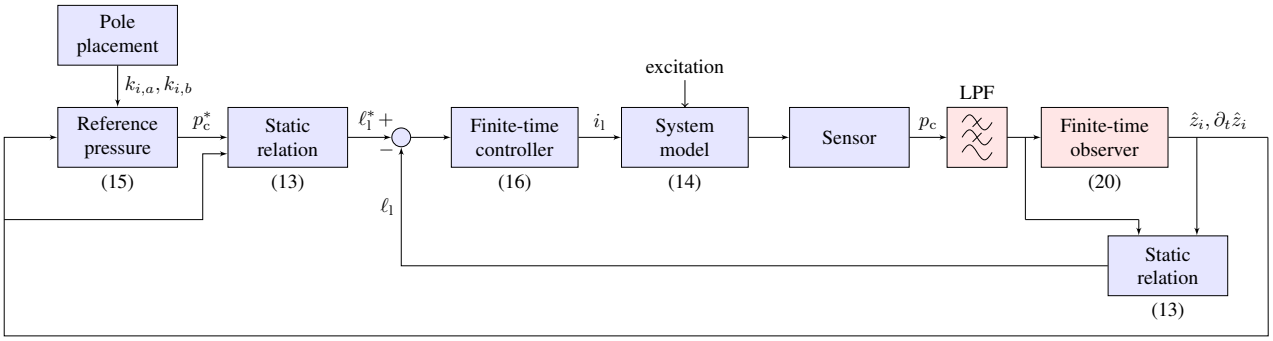

Figure 5. Control layout with observer-regulator and low-pass filter (LPF). Corresponding equations are indicated.

For the linear system (14), one could use a standard Luenberger observer [33] of the form

$$\dot{\hat{\boldsymbol{x}}} = \boldsymbol{A}\hat{\boldsymbol{x}} + \boldsymbol{B}u + \boldsymbol{L}(y - \boldsymbol{C}\hat{\boldsymbol{x}}). \tag{17}$$

The state estimate $\hat{\boldsymbol{x}}$ converges to the real (unknown) state $\boldsymbol{x}$ by copying the system dynamics and by correcting for the error between the measured system output y and the estimated output $\boldsymbol{C}\hat{\boldsymbol{x}}$ weighted by a matrix $\boldsymbol{L}$ designed by a pole placement. There typically exists a trade-off between fast convergence of the observer and its robustness to noise.

In the present work, we have chosen to design a finite-time (nonlinear) observer instead, that is presented in following Lemma.

Lemma 1 (Finite-time observer [34])**.** *Consider a nonlinear system*

$$\begin{cases} \dot{\boldsymbol{x}} = \boldsymbol{\eta}(\boldsymbol{x}, \boldsymbol{u}) \\ y = h(\boldsymbol{x}) \end{cases} \tag{18}$$

with $\boldsymbol{x} \in \mathbb{R}^n, \boldsymbol{u} \in \mathbb{R}^m$ that is locally observable and assume there exists a local state coordinate transformation that transforms it into the canonical observable form

$$\begin{cases} \dot{\boldsymbol{z}} = \boldsymbol{A}^\circ \boldsymbol{z} + \boldsymbol{f}(y, \boldsymbol{u}, \dot{\boldsymbol{u}}, \ldots, \boldsymbol{u}^{(r)}) \\ y = \boldsymbol{C}^\circ \boldsymbol{z} \end{cases}$$

with

$$\boldsymbol{A}^\circ = \begin{bmatrix} a_1 & 1 & 0 & \ldots & 0 \\ a_2 & 0 & 1 & \ldots & 0 \\ \vdots & \vdots & \vdots & \ddots & \vdots \\ a_{n-1} & 0 & 0 & \ldots & 1 \\ a_n & 0 & 0 & \ldots & 0 \end{bmatrix}, \; \boldsymbol{C}^\circ = \begin{bmatrix} 1 & 0 & \ldots & 0 \end{bmatrix},$$

and a new state $\boldsymbol{z} \in \mathbb{R}^n$. Then there exists a number $\varepsilon \in [1 - \frac{1}{n-1}, 1[$ such that the system

$$\dot{\hat{\boldsymbol{z}}} = \boldsymbol{A}^\circ \hat{\boldsymbol{z}} + \boldsymbol{f}(y, \boldsymbol{u}, \dot{\boldsymbol{u}}, \ldots, \boldsymbol{u}^r) + \begin{bmatrix} h_1 \lfloor y - \boldsymbol{C}^\circ \hat{\boldsymbol{z}} \rceil^{\theta_1} \\ \vdots \\ h_n \lfloor y - \boldsymbol{C}^\circ \hat{\boldsymbol{z}} \rceil^{\theta_n} \end{bmatrix} \tag{19}$$

with parameters $\theta_i = i\theta - (i-1)$, $\theta \in]1 - \varepsilon, 1[$ and gains h_i such that the matrix

$$\begin{bmatrix} -h_1 & 1 & 0 & \ldots & 0 \\ -h_2 & 0 & 1 & \ldots & 0 \\ \vdots & \vdots & \vdots & \ddots & \vdots \\ -h_{n-1} & 0 & 0 & \ldots & 1 \\ -h_n & 0 & 0 & \ldots & 0 \end{bmatrix}$$

is Hurwitz, is a finite-time observer of the system (18)*.*

In the case of the linear system (14), we have $\boldsymbol{f}(y, \boldsymbol{u}, \dot{\boldsymbol{u}}, \ldots, \boldsymbol{u}^r) = \boldsymbol{B}\boldsymbol{u}$. We now express the finite-time observer (19) in the original coordinates of the linear system (14).

Lemma 2 (Transformation to original coordinates)**.** *The finite-time observer* (19) *defined in Lemma 1 is expressed in the original coordinates as*

$$\dot{\hat{\boldsymbol{x}}} = \boldsymbol{A}\hat{\boldsymbol{x}} + \boldsymbol{B}\boldsymbol{u} + \boldsymbol{P}\boldsymbol{Q} \begin{bmatrix} h_1 \lfloor y - \boldsymbol{C}\hat{\boldsymbol{x}} \rceil^{\theta_1} \\ \vdots \\ h_n \lfloor y - \boldsymbol{C}\hat{\boldsymbol{x}} \rceil^{\theta_n} \end{bmatrix}. \tag{20}$$

This formula contains two state transformation matrices:

$$\boldsymbol{P} = \begin{bmatrix} \boldsymbol{H} & \boldsymbol{A}\boldsymbol{H} & \ldots & \boldsymbol{A}^{n-1}\boldsymbol{H} \end{bmatrix},$$

where $\boldsymbol{H} = \boldsymbol{\mathcal{O}}^{-1} \begin{bmatrix} 0 & \ldots & 0 & 1 \end{bmatrix}^\intercal$ is the last column of the inverse of the observability matrix $\boldsymbol{\mathcal{O}} = \begin{bmatrix} (\boldsymbol{C})^\intercal & (\boldsymbol{C}\boldsymbol{A})^\intercal & \ldots & (\boldsymbol{C}\boldsymbol{A}^{n-1})^\intercal \end{bmatrix}^\intercal$ of the linear system (14)*, and*

$$\boldsymbol{Q} = \begin{bmatrix} 0 & 0 & 1 \\ 0 & \iddots & 0 \\ 1 & 0 & 0 \end{bmatrix}.$$

Proof. The state transformation matrix $\boldsymbol{P}$ as defined in [33] enables to perform a similarity transform, bringing the system (14) in an alternative observable canonical form, differing from the observable canonical form used in Lemma 1 by a permutation expressed by the permutation matrix $\boldsymbol{Q}$. Applying the inverse state transformations and similarity transforms to the finite-time observer (19) yields the form (20) in the original coordinates. □

Applying the finite-time observer to a linear system (20) gives a similar structure as the classical Luenberger observer (17), the correction term $\boldsymbol{L}(y - \boldsymbol{C}\hat{\boldsymbol{x}})$ of which being

replaced by a nonlinear expression. It is this nonlinear expression that guarantees a finite-time convergence of the observer, rather than an asymptotical convergence.

4.2 Simulation

The previous control case is reconsidered, where the state used in the control law is now observed based on the measurement of the cavity pressure $\tilde{p}_{\mathrm{c}}^{\mathrm{m}}$. The observer parameters are $\theta = 0.95$, $\begin{bmatrix} h_1 & \dots & h_6 \end{bmatrix} = \begin{bmatrix} 13.5 & 73.75 & 208.125 & 319 & 250.875 & 78.75 \end{bmatrix}$. As shown in Fig. 6, after an initial transient due to the convergence of the observer, one obtains the same frequencies $\tilde{f}_1$ and $\tilde{f}_2$ as in the simulation in Subsection 3.4.

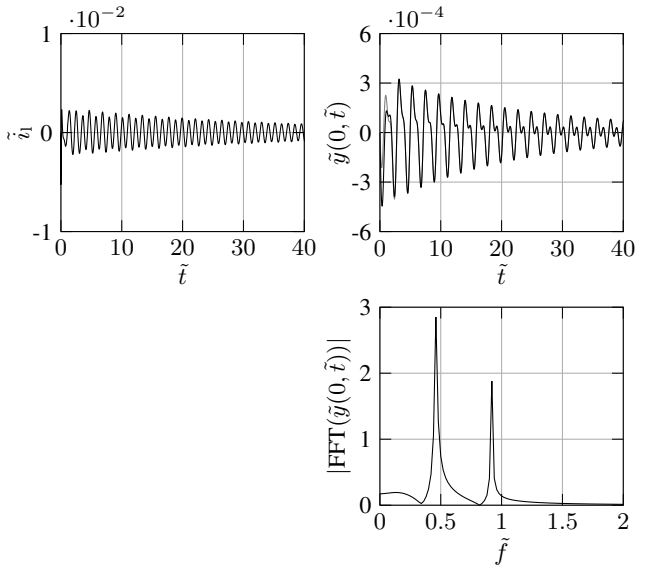

Figure 6. Simulation of the system with $N = 2$ modes controlled by the observer-regulator. The gray line shows the obtained observation of $\tilde{y}(0, \tilde{t})$.

5. SPILLOVER

5.1 Concept

The presentation of the proposed observer-regulator is concluded with some additional remarks with a view to a practical implementation.

In the design of the observer-regulator, a finite number of modes N is considered. The resulting control law is then applied to the physical system containing an infinite number of modes. Two types of so-called spillover can occur: the control law potentially excites higher-frequency modes which could lead to instability (control spillover), and higher-frequency modes are present in the measured system outputs, influencing the observer behaviour (observer spillover).

Two remarks can be mentioned, that are based on a local linear approximation of the closed loop system. Firstly, stability in presence of control spillover can be guaranteed by proving that the uncontrolled higher-frequency modes have a bounded energy [35]. Secondly, in order to reduce observer spillover, a low-pass filter is added in the control loop (Fig. 5), as proposed in [36]. In this way, only the lower frequencies corresponding to the considered first N modes in the observer-regulator are taken into account and fed back to the system.

A more thorough discussion of nonlinear spillover effects and their influence on the finite-time property of the closed loop system is beyond the scope of this paper.

5.2 Simulation

The previously simulated observer-regulator considering the first 2 modes is applied to the model (14) with 7 modes, inducing thereby spillover effects due to the presence of several higher-frequency modes. The model has zero initial conditions except for $\partial_{\tilde{t}} \tilde{z}_i = -0.001$ for all 7 modes.

The result is compared to the case without control in Fig. 7. In this example, the spillover effects did not provoke an instability of the closed loop system. Nonetheless, the mentioned low-pass filter could stil be added in the control loop in order to reduce possible control performance deterioration caused by the presence of unmodeled higher-frequency modes. Attention must be paid to the group delay of the filter, that could be a cause of instability of the closed loop system.

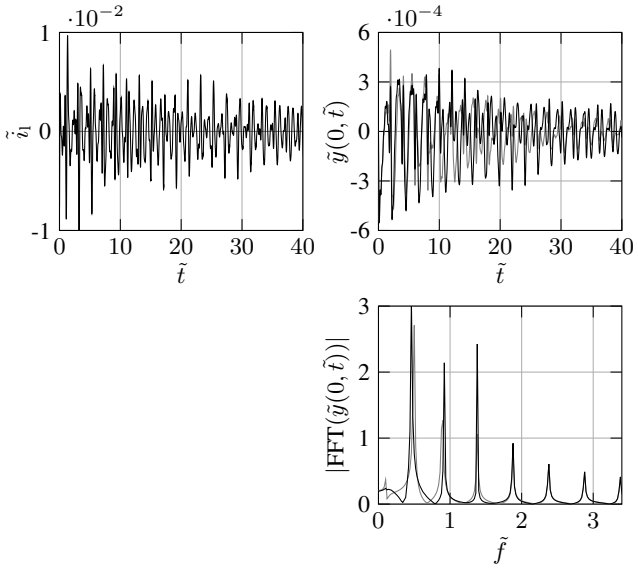

Figure 7. Simulation of the system with 7 modes without control (gray) and with the observer-regulator considering the first 2 modes (black).

6. CONCLUSION AND FUTURE WORKS

We have designed an observer-regulator that is able to modify the frequencies of N vibration modes of a tom-tom membrane, using only a measurement of the pressure inside the drum cavity. Some relevant aspects towards a practical implementation were mentioned. We wish to implement the controller on a testbench that is under construction.

7. ACKNOWLEDGEMENTS

BdAN and MW are supported by ANR project Finite4SoS (ANR 15 CE23 0007). TH, DR and MW acknowledge ANR-DFG project INFIDHEM (ANR 16 CE92 0028).

8. REFERENCES

[1] S. J. Elliott and P. A. Nelson, "Active noise control," *IEEE signal processing magazine*, vol. 10, no. 4, pp. 12–35, 1993.

[2] C. C. Fuller, S. Elliott, and P. A. Nelson, *Active control of vibration*. Academic Press, 1996.

[3] B. d'Andréa-Novel, B. Fabre, and J.-M. Coron, "An acoustic model for automatic control of a slide flute," *Acta Acustica united with Acustica*, vol. 96, no. 4, pp. 713–721, 2010.

[4] H. Boutin, *Méthodes de contrôle actif d'instruments de musique. Cas de la lame de xylophone et du violon.* PhD thesis, Université Pierre et Marie Curie – Paris VI, 2011.

[5] S. Benacchio, *Contrôle actif modal appliqué aux instruments de musique à cordes*. PhD thesis, Université Pierre et Marie Curie – Paris VI, 2014.

[6] T. Meurisse, *Contrôle Actif Appliqué aux Instruments de Musique à Vent*. PhD thesis, Université Pierre et Marie Curie – Paris VI, 2014.

[7] M. Jossic, A. Mamou-Mani, B. Chomette, D. Roze, F. Ollivier, and C. Josserand, "Modal active control of Chinese gongs," *The Journal of the Acoustical Society of America*, vol. 141, no. 6, pp. 4567–4578, 2017.

[8] S. Z. Solomon, *How to write for Percussion: a comprehensive guide to percussion composition*. Oxford University Press, 2016.

[9] R. S. Christian, R. E. Davis, A. Tubis, C. A. Anderson, R. I. Mills, and T. D. Rossing, "Effects of air loading on timpani membrane vibrations," *The Journal of the Acoustical Society of America*, vol. 76, no. 5, pp. 1336–1345, 1984.

[10] A. Chaigne and J. Kergomard, *Acoustics of musical instruments*. Springer, 2016.

[11] J. D. Rollow IV, *Active Control of Spectral Detail Radiated by an air-loaded impacted membrane*. PhD thesis, The Pennsylvania State University, 2003.

[12] M. Lupone and L. Seno, "Gran cassa and the adaptive instrument feed-drum," in *International Symp. on Computer Music Modeling and Retrieval*, pp. 149–163, Springer, 2005.

[13] M. Van Walstijn and P. Rebelo, "The prosthetic conga: Towards an actively controlled hybrid musical instrument," in *ICMC*, Citeseer, 2005.

[14] J. Gregorio and Y. Kim, "Augmentation of acoustic drums using electromagnetic actuation and wireless control," *Journal of the Audio Engineering Society*, vol. 66, no. 4, pp. 202–210, 2018.

[15] D. Rector and S. Topel, "EMdrum: An Electromagnetically Actuated Drum," in *Proc. of NIME*, pp. 395–398, 2014.

[16] P. Williams and D. Overholt, "Design and evaluation of a digitally active drum," *Personal and Ubiquitous Computing*, 2020.

[17] S. P. Bhat and D. S. Bernstein, "Finite-time stability of continuous autonomous systems," *SIAM Journal on Control and Optimization*, vol. 38, no. 3, pp. 751–766, 2000.

[18] M. Wijnand, B. d'Andréa-Novel, B. Fabre, T. Hélie, L. Rosier, and D. Roze, "Active control of the axisymmetric vibration modes of a tom-tom drum," in *2019 IEEE 58th Conference on Decision and Control (CDC)*, IEEE, 2019.

[19] K. F. Graff, *Wave motion in elastic solids*. Courier Corporation, 2012.

[20] L. E. Kinsler, A. R. Frey, A. B. Coppens, and J. V. Sanders, *Fundamentals of acoustics*. Wiley, 1999 (4th edition).

[21] P. M. Morse, *Vibration and sound*. American Society of Acoustics, 1995.

[22] B. M. Maschke and A. J. van der Schaft, "Port-controlled Hamiltonian systems: modelling origins and systemtheoretic properties," *IFAC Proc. Volumes*, vol. 25, no. 13, pp. 359–365, 1992.

[23] A. van der Schaft, "Port-Hamiltonian systems: an introductory survey," in *Proc. of the international congress of mathematicians*, vol. 3, pp. 1339–1365, Citeseer, 2006.

[24] A. Falaize and T. Hélie, "Passive Guaranteed Simulation of Analog Audio Circuits: A Port-Hamiltonian Approach," *Applied Sciences*, vol. 6, no. 10, p. 273, 2016.

[25] R. Ortega, A. van der Schaft, B. Maschke, and G. Escobar, "Interconnection and damping assignment passivity-based control of port-controlled Hamiltonian systems," *Automatica*, vol. 38, no. 4, pp. 585–596, 2002.

[26] R. F. Curtain and H. Zwart, *An Introduction to Infinite-Dimensional Linear Systems Theory*. Springer, 1995.

[27] T. Hélie and D. Matignon, "Nonlinear damping models for linear conservative mechanical systems with preserved eigenspaces: a port-Hamiltonian formulation," *IFAC-PapersOnLine*, vol. 48, no. 13, pp. 200–205, 2015.

[28] J. A. Villegas, *A Port-Hamiltonian Approach to Distributed Parameter Systems*. PhD thesis, University of Twente, 2007.

[29] A. C. Hindmarsh, "ODEPACK, a systematized collection of ODE solvers," *IMACS Transactions on Scientific Computation*, vol. 1, pp. 55–64, 1983.

[30] M. Wijnand, B. d'Andréa-Novel, T. Hélie, and D. Roze, "Contrôle des vibrations d'un oscillateur passif : stabilisation en temps fini et par remodelage d'énergie," in *Congrès Français d'Acoustique*, 2018.

[31] T. Lebrun, M. Wijnand, T. Hélie, D. Roze, and B. d'Andréa-Novel, "Electroacoustic Absorbers Based on Passive Finite-Time Control of Loudspeakers: A Numerical Investigation," in *Nonlinear Dynamics and Control (Rome)*, pp. 23–31, Springer International Publishing, 2020.

[32] E. Bernuau, W. Perruquetti, D. Efimov, and E. Moulay, "Robust finite-time output feedback stabilisation of the double integrator," *International Journal of Control*, vol. 88, no. 3, pp. 451–460, 2015.

[33] B. d'Andréa-Novel and M. C. de Lara, *Commande linéaire des systèmes dynamiques*. Masson, 1994.

[34] W. Perruquetti, T. Floquet, and E. Moulay, "Finite-time observers: application to secure communication," *IEEE Transactions on Automatic Control*, vol. 53, no. 1, pp. 356–360, 2008.

[35] M. J. Balas, "Modal control of certain flexible dynamic systems," *SIAM Journal on Control and Optimization*, vol. 16, no. 3, pp. 450–462, 1978.

[36] M. J. Balas, "Feedback control of flexible systems," *IEEE Transactions on Automatic Control*, vol. 23, no. 4, pp. 673–679, 1978.